

file as NACA-TR-534



**NATIONAL ADVISORY COMMITTEE  
FOR AERONAUTICS**

**REPORT No. 534**

**AERODYNAMIC CHARACTERISTICS OF A WING  
WITH FOWLER FLAPS INCLUDING FLAP LOADS  
DOWNWASH, AND CALCULATED EFFECT  
ON TAKE-OFF**

**By ROBERT C. PLATT**



**1935**

REPRODUCED BY  
**NATIONAL TECHNICAL  
INFORMATION SERVICE**  
U. S. DEPARTMENT OF COMMERCE  
SPRINGFIELD, VA. 22161

# AERONAUTIC SYMBOLS

## FUNDAMENTAL AND DERIVED UNITS

Name	Symbol	Unit	Conversion Factor
Length	m	metre	3.28084 ft.
Area	m <sup>2</sup>	square metre	10.7639 sq. ft.
Volume	m <sup>3</sup>	cubic metre	35.3147 cu. ft.
Force	N	newton	0.22481 lb.
Weight	kg	kilogram	2.20462 lb.
Velocity	m/s	metre per second	2.23694 mph
Acceleration	m/s <sup>2</sup>	metre per second squared	3.28084 ft./s <sup>2</sup>
Angular Velocity	rad/s	radian per second	57.2958 deg./s
Angular Acceleration	rad/s <sup>2</sup>	radian per second squared	57.2958 deg./s <sup>2</sup>
Power	W	watt	0.737562 hp
Energy	J	joule	0.737562 ft.-lb.
Work	J	joule	0.737562 ft.-lb.
Heat	J	joule	0.737562 ft.-lb.
Temperature	K	kelvin	1.8 °F
Pressure	N/m <sup>2</sup>	newton per square metre	0.000145038 psi
Dynamic Pressure	N/m <sup>2</sup>	newton per square metre	0.000145038 psi
Stagnation Pressure	N/m <sup>2</sup>	newton per square metre	0.000145038 psi
Static Pressure	N/m <sup>2</sup>	newton per square metre	0.000145038 psi
Temperature	K	kelvin	1.8 °F
Temperature	°C	degree Celsius	1.8 °F
Temperature	°F	degree Fahrenheit	1.8 °C

## GENERAL SYMBOLS

- 1.  $\rho$  Density (mass per unit volume)
- 2.  $\rho_0$  Standard density of dry air, 0.12497 kg/m<sup>3</sup> at 15° C and 760 mm, or 0.002378 lb./ft.<sup>3</sup> sec.
- 3.  $\sigma$  Specific weight of standard air, 1.2258 kg/m<sup>3</sup> or 0.0765 lb./cu. ft.
- 4.  $\alpha$  Angle of setting of wing relative to thrust line
- 5.  $\beta$  Angle of stabilizer setting relative to thrust line
- 6.  $M$  Resultant moment
- 7.  $\omega$  Resultant angular velocity
- 8.  $Re$  Reynolds Number, where  $l$  is a linear dimension (e.g.  $l = 200$  mm model airfoil,  $l = 100$  in. chord, 100 m.p.h. normal pressure at 15° C, the corresponding number is 224,000) or for a model of length  $l$  in air of density  $\rho$  and viscosity  $\mu$ ,  $Re = \frac{\rho V l}{\mu}$
- 9.  $x/c$  Ratio of pressure coefficient (ratio of distance of  $x$  from leading edge to chord length)
- 10.  $\alpha_i$  Angle of attack
- 11.  $\alpha_d$  Angle of downwash
- 12.  $\alpha_{cr}$  Angle of attack, critical angle of stall
- 13.  $\alpha_{st}$  Angle of attack, stall angle
- 14.  $\alpha_{tr}$  Angle of attack, transition angle of stall
- 15.  $\alpha_{pr}$  Angle of attack, practical angle of stall
- 16.  $\alpha_{max}$  Angle of attack, maximum angle of stall

## NOTICE

THIS DOCUMENT HAS BEEN REPRODUCED FROM THE BEST COPY FURNISHED US BY THE SPONSORING AGENCY. ALTHOUGH IT IS RECOGNIZED THAT CERTAIN PORTIONS ARE ILLEGIBLE, IT IS BEING RELEASED IN THE INTEREST OF MAKING AVAILABLE AS MUCH INFORMATION AS POSSIBLE.



---

---

**REPORT No. 534**

---

**AERODYNAMIC CHARACTERISTICS OF A WING  
WITH FOWLER FLAPS INCLUDING FLAP LOADS  
DOWNWASH, AND CALCULATED EFFECT  
ON TAKE-OFF**

**By ROBERT C. PLATT**  
**Langley Memorial Aeronautical Laboratory**

# NATIONAL ADVISORY COMMITTEE FOR AERONAUTICS

HEADQUARTERS, NAVY BUILDING, WASHINGTON, D. C.

LABORATORIES, LANGLEY FIELD, VA.

Created by act of Congress approved March 3, 1915, for the supervision and direction of the scientific study of the problems of flight. Its membership was increased to 15 by act approved March 2, 1929. The members are appointed by the President, and serve as such without compensation.

JOSEPH S. AMES, Ph. D., *Chairman*,  
President, Johns Hopkins University, Baltimore, Md.

DAVID W. TAYLOR, D. Eng., *Vice Chairman*,  
Washington, D. C.

CHARLES G. ABBOT, Sc. D.,  
Secretary, Smithsonian Institution.

LYMAN J. BRIGGS, Ph. D.,  
Director, National Bureau of Standards.

BENJAMIN D. FOULLOIS, Major General, United States Army,  
Chief of Air Corps, War Department.

WILLIS RAY GREGG, B. A.,  
Chief, United States Weather Bureau.

HARRY F. GUGGENHEIM, M. A.,  
Port Washington, Long Island, N. Y.

ERNEST J. KING, Rear Admiral, United States Navy,  
Chief, Bureau of Aeronautics, Navy Department.

CHARLES A. LINDBERGH, LL. D.,  
New York City.

WILLIAM P. MACCRACKEN, Jr., Ph. B.,  
Washington, D. C.

AUGUSTINE W. ROBINS, Brig. Gen., United States Army,  
Chief, Matériel Division, Air Corps, Wright Field, Dayton,  
Ohio.

EUGENE L. VIDAL, C. E.,  
Director of Air Commerce, Department of Commerce.

EDWARD P. WARNER, M. S.,  
Editor of Aviation, New York City.

R. D. WEYERBACHER, Commander, United States Navy,  
Bureau of Aeronautics, Navy Department.

ORVILLE WRIGHT, Sc. D.,  
Dayton, Ohio.

---

GEORGE W. LEWIS, *Director of Aeronautical Research*

JOHN F. VICTORY, *Secretary*

HENRY J. E. REID, *Engineer in Charge, Langley Memorial Aeronautical Laboratory, Langley Field, Va.*

JOHN J. IDE, *Technical Assistant in Europe, Paris, France*

---

## TECHNICAL COMMITTEES

AERODYNAMICS  
POWER PLANTS FOR AIRCRAFT  
AIRCRAFT STRUCTURES AND MATERIALS

AIRCRAFT ACCIDENTS  
INVENTIONS AND DESIGNS

*Coordination of Research Needs of Military and Civil Aviation*

*Preparation of Research Programs*

*Allocation of Problems*

*Prevention of Duplication*

*Consideration of Inventions*

LANGLEY MEMORIAL AERONAUTICAL LABORATORY  
LANGLEY FIELD, VA.

Unified conduct, for all agencies, of scientific research on the fundamental problems of flight.

OFFICE OF AERONAUTICAL INTELLIGENCE  
WASHINGTON, D. C.

Collection, classification, compilation, and dissemination of scientific and technical information on aeronautics.

## REPORT No. 534

### AERODYNAMIC CHARACTERISTICS OF A WING WITH FOWLER FLAPS INCLUDING FLAP LOADS, DOWNWASH, AND CALCULATED EFFECT ON TAKE-OFF

By ROBERT C. PLATT

#### SUMMARY

*This report presents the results of an investigation in the N. A. C. A. 7- by 10-foot wind tunnel on a wing in combination with each of three sizes of Fowler flap. The purpose of the investigation was to determine the aerodynamic characteristics as affected by flap chord and position, the air loads on the flaps, and the effect of the flaps on the downwash. The flap position for maximum lift; polars for arrangements considered favorable for take-off; and complete lift, drag, and pitching-moment characteristics for selected optimum arrangements were determined. A Clark Y wing model was tested with 20 percent  $c$ , 30 percent  $c$ , and 40 percent  $c$  Fowler flaps of Clark Y section. Certain additional data from earlier tests on a similar model equipped with the 40 percent  $c$  Clark Y flap are included for comparison. Results of calculations made to find the effect of the Fowler flap on take-off, based on data from these tests, are included in an appendix.*

*The maximum lift coefficient obtainable, based on original wing area, had a nearly linear increase with flap chord up to 40 percent, but the maximum lift force per unit of total area increased very little beyond the value obtained with the 30 percent  $c$  flap. The maximum load on the flap occurred very nearly at the maximum lift of the wing-flap combination and was nearly  $1\frac{1}{2}$  times the load that would result from uniform distribution of the total load over the total area. In general, the flap appeared to carry a large proportion of the additional lift caused by its presence and to have its center of pressure much nearer the leading edge than it would normally be in free air. The addition of the Fowler flap to a wing appeared to have no appreciable effect on the relation between lift coefficient and angle of downwash. The calculations in the appendix show that, by proper use of the Fowler flap, the take-off of an airplane having wing and power loadings in the range normally encountered in transport airplanes should be considerably improved.*

#### INTRODUCTION

During the past few years the use of flaps on high-performance airplanes as a device for reducing space required in landing has become common. Thus far split flaps have been most generally used, probably

because of their simplicity of application and their superiority in giving steep gliding approaches and short landing runs: the features of flaps with which designers have been most concerned. In order to retain satisfactory operation from normal flying fields with fast airplanes, however, the use of high-lift devices that improve take-off as well as landing is desirable. Since drag is unfavorable to take-off, the comparatively large drag of split flaps places them among the least promising of high-lift devices in this respect. The Fowler flap appears to offer a better compromise between these conflicting requirements. For equal sizes it will give higher maximum lift with no higher profile drag than most other flap arrangements and its comparatively low drag at high lifts is favorable to take-off and steep climb. This effect would normally entail some sacrifice of steep gliding ability.

Although sufficient data to form some estimate of the performance to be expected from an airplane equipped with Fowler flaps are available (references 1 and 2), they are inadequate for normal design purposes. The purpose of the tests reported herein is to provide data to form a rational basis for the design of airplanes equipped with Fowler flaps. It appears that for the present the purpose will be attained by making available the following information: effect of flap size on aerodynamic characteristics attainable, aerodynamic loads applied to the flap in various conditions, and effect of the flap on downwash. In addition, a convenient method of estimating the effect of high-lift devices on airplane take-off should prove of assistance in cases where this performance feature merits special attention.

The tests were made in the 7- by 10-foot wind tunnel of the N. A. C. A. (reference 3) at Langley Field, Va., during the summer and fall of 1934.

#### MODEL

The basic wing was built of laminated mahogany to the Clark Y profile (table I) and had a span of 60 inches and a chord of 10 inches. The trailing edge was cut away and the upper surface replaced by a thin curved metal plate. The lower surface was left open at the rear to serve as a retracting well for the flaps.

Blocks were inserted to maintain the correct size of well for each size of flap tested. Figure 1 shows the profile of the wing with the various flaps in place.

The two smaller flaps were made of duralumin to the Clark Y profile and had spans of 60 inches and chords of 2 and 3 inches. The largest flap, which is the one described in reference 2, was made of mahogany and had a 4-inch chord. The flaps were supported on the wing by fittings attached to ribs located in the retracting well. Several sets of attachment holes in the ribs, combined with several sets of fittings, gave the range of flap positions shown in figure 1. The flaps were supported on the fittings by hinges located at the center of the leading-edge arc of the flaps, angular adjustment being obtained by set screws attached to

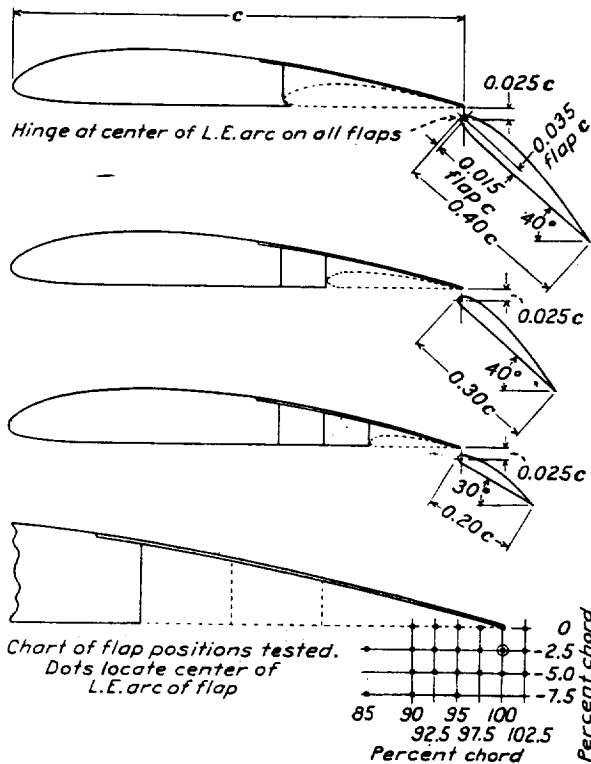


FIGURE 1.—Wing with various Fowler flaps. Flaps shown in maximum-lift conditions.

the flap moving in quadrantal slots in the fittings. In general, where the term "flap position" is used, the position of the flap hinge axis is indicated, irrespective of angle, and flap angle is measured between the chord lines of the wing and the flap.

#### TESTS

Five groups of tests were made in obtaining the data presented in this report. These five groups dealt with maximum lift, optimum flap arrangement for take-off, standard force tests of optimum arrangements, flap loads, and downwash behind the wing with various flap arrangements.

**Maximum lift.**—The maximum lift coefficients obtainable with the 0.20  $c$  and 0.30  $c$  flaps at various

positions shown in figure 1 were found by tests in which the flap angle was increased from 20° in 10° steps until the peak of the variation of  $C_{L_{max}}$  with flap angle was defined for each position. The range of positions in both cases was sufficient to surround the point at which the highest lift coefficient was found, thus isolating an optimum position in each case. Similar surveys had previously been made with the 0.40  $c$  flap (reference 2) and were not repeated at this time.

**Optimum take-off arrangement.**—Lift and drag data were taken at a range of flap angles between 0° and that giving maximum lift for a series of flap positions somewhat more restricted than the range used in the maximum-lift tests. Care was exercised in these tests also to surround what was judged to be the optimum setting, both as regards position and angle.

**Standard force tests of optimum arrangements.**—A series of final force tests, consisting of lift, drag, and pitching-moment measurements, was made at the flap positions considered to be of special interest. These included tests of the maximum-lift arrangement of each flap, of the optimum take-off arrangement of each flap, and of an arbitrarily selected arrangement representing partial retraction of each flap.

All tests in these first three groups were conducted in accordance with standard force-test procedure as described in reference 3.

**Flap loads.**—Air loads acting on the flaps were found by supporting the flaps independently of the wing, at the same position and angle as used in the final force tests of the wing-flap combinations, and by measuring the forces on the wing alone in the presence of the flap. The flap loads could then be readily computed. In order to find the center of pressure of the load on the flap, the flap hinge moment was measured by observing the angular deflection of a long slender torque rod required to balance the flap at the angle in question. Similar measurements of loads and center-of-pressure locations on split flaps are more completely described in reference 4.

**Downwash.**—Measurements were made with "pitot-yaw" tubes attached to the wing by a rigid support. The reference position thus moved in the air stream as the angle of attack was changed but remained the same with respect to the wing, as does the tail of an airplane. The angles of downwash, however, were referred to the initial direction of the free air stream. The apparatus could be adjusted to various horizontal distances behind the wing. The pitot-yaw tubes were ordinary round-nosed pitot tubes with two additional nose holes at 45° above and below the tube axis. Alcohol manometers were used to read the pressures, and the tubes were calibrated in test position in the clear-tunnel air stream.

The wind tunnel is of the open jet, closed return type, with a rectangular jet 7 by 10 feet in size. A

complete description of the tunnel, balance, and standard force-test procedure appears in reference 3.

Tests were run at a dynamic pressure of 16.37 pounds per square foot, corresponding to an air speed of 80 miles per hour at standard sea-level conditions. The Reynolds Number of the tests, based on the 10-inch chord of the wing without flaps, was approximately 609,000.

**PRECISION**

The accidental errors in the results presented in this report are believed to lie within the limits indicated in the following table:

Wing data	Flap load data	Downwash data
$\alpha$ ..... $\pm 0.10^\circ$	$C_{N_f}$ ..... $\pm 0.10$	$\epsilon$ ..... $\pm 0.5^\circ$
$C_{L_{max}}$ ..... $\pm 0.5$	$C_{x_f}$ ..... $\pm 0.06$	
$C_{m_{c-f}}$ ..... $\pm 0.008$	$C_{h_f}$ ..... $\pm 0.004$	
$C_D$ ( $C_L=1$ )..... $\pm 0.001$	Flap angle..... $\pm .25^\circ$	
$C_D$ ( $C_L=1$ )..... $\pm 0.004$	Flap position..... $\pm 0.03 c$	
$C_D$ ( $C_L=2$ )..... $\pm 0.008$		
Flap angle..... $\pm .25^\circ$		
Flap position..... $\pm 0.015 c$		

Consistent differences between results obtained in the 7- by 10-foot wind tunnel and in free air may be ascribed to effects of the following factors: Jet boundaries, static-pressure gradient, turbulence, and scale. In order that the present results be consistent with published results of tests of other high-lift devices in the 7- by 10-foot tunnel, no corrections for these effects have been made. Corrections of several sets of airfoil results have indicated that the values of the jet-boundary correction factors,  $\delta_a = -0.165$ , and  $\delta_D = -0.165$ , used in the standard equations (cf. reference 5) are satisfactory for a 10-inch by 60-inch wing. The static pressure in the jet decreases downstream, producing an increment in  $C_D$  of 0.0015 on normal 12 percent  $c$  thick rectangular airfoils. Evidence at present available indicates that the effect of the turbulence in this tunnel is small as compared with the other consistent errors.

**RESULTS AND DISCUSSION**

All test results are given in standard nondimensional coefficient form. In the case of a wing with a retractable surface, the convention of basing coefficients on the area that would be exposed in normal flight, that is, the minimum area, has been adopted. The coefficients used are then defined as follows:

- subscript  $w$  refers to the basic wing
- subscript  $f$  refers to the flap
- $q = \frac{1}{2} \rho V^2$
- $C_L = \frac{\text{lift}}{S_w q}$
- $C_D = \frac{\text{drag}}{S_w q}$
- $C_m = \frac{\text{pitching moment}}{C_{m_f} S_w q}$
- normal force on flap (perpendicular to flap chord)
- $C'_{x_f} = \frac{\text{longitudinal force on flap (along flap chord)}}{S_f q}$
- $C_{h_f} = \frac{\text{flap hinge moment}}{S_f c_f q}$

$$C'_{x_f} = \frac{\text{longitudinal force on flap (along flap chord)}}{S_f q}$$

$$C_{h_f} = \frac{\text{flap hinge moment}}{S_f c_f q}$$

$\epsilon$ , angle of downwash, degrees.

**Maximum-lift condition.**—The results of the maximum-lift tests are presented as contours showing variations of  $C_{L_{max}}$  with flap hinge position, irrespective of flap angle. Figures 2, 3, and 4 show contours

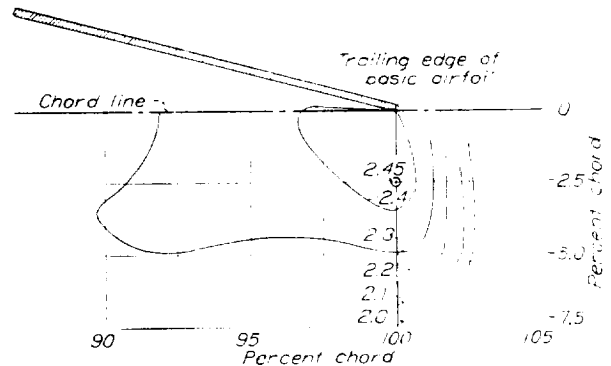


FIGURE 2.—Contours showing variation of  $C_{L_{max}}$  with flap position. 0.20  $c$  flap.

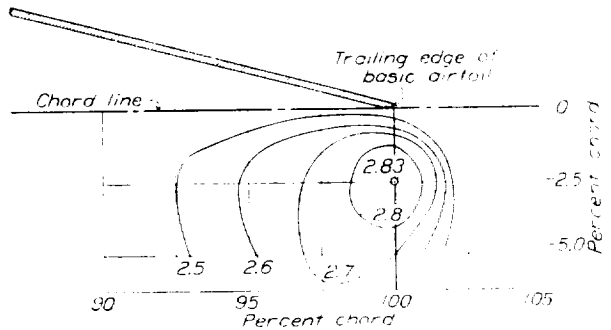


FIGURE 3.—Contours showing variation of  $C_{L_{max}}$  with flap position. 0.30  $c$  flap.

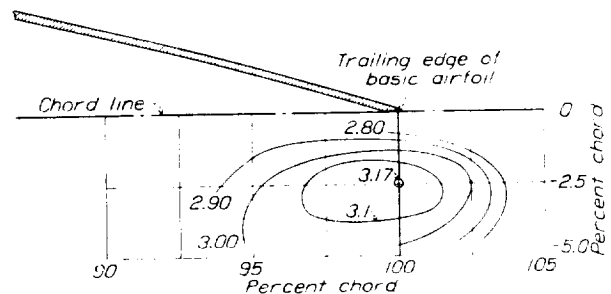


FIGURE 4.—Contours showing variation of  $C_{L_{max}}$  with flap position. 0.40  $c$  flap (data from N. A. C. A., T. N. No. 419).

for the 20 percent chord, 30 percent chord, and 40 percent chord flaps, respectively. Data on the 40 percent chord flap are taken from reference 2, no further tests having been considered necessary on that size of flap after an analysis was made of the data for the two smaller flaps. The optimum position is the same for all three flaps: 2.5 percent of the main wing chord directly below the trailing edge. The optimum angle was  $30^\circ$  for the 20 percent  $c$  flap and  $40^\circ$  for the two larger flaps.

Variation of  $C_{L_{max}}$  with flap size is shown in figure 5. The maximum lift coefficient increases approximately in proportion to flap size if the area of only the original wing is considered. This is a reasonably satisfactory basis for comparison of the landing speeds of an airplane with various sizes of flap if a constant maximum speed is maintained. If the maximum lift force that a wing will give at a certain air speed per unit of structural weight is taken as a criterion, it is reasonable to compare the various sizes of flap on the basis of total

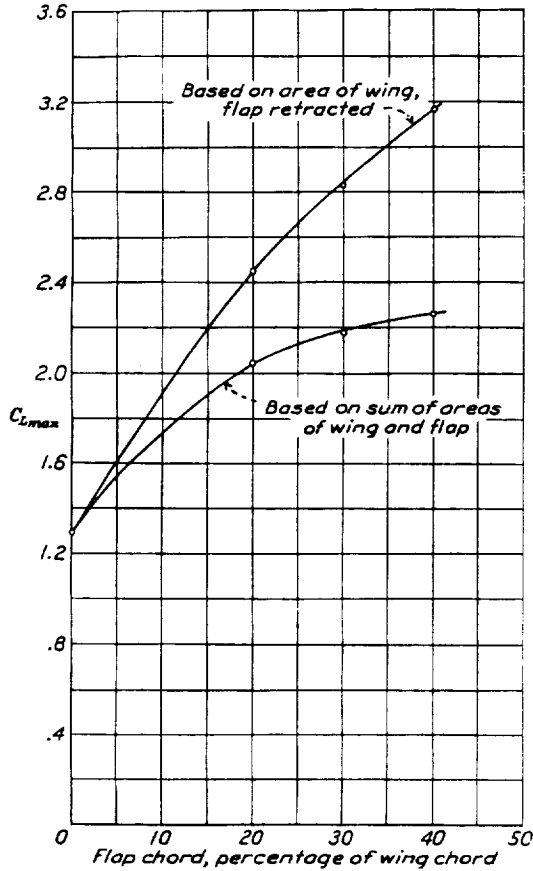


FIGURE 5.—Variation of  $C_{L_{max}}$  with flap size. Flap set at optimum position and angle.

(wing-and-flap) area. On this basis there is clearly little to be gained by using flaps larger than 30 percent  $c$ .

Lift, drag, and pitching-moment data for the wing with each of the three flap sizes, with the flap at the setting for maximum lift, are given in figure 6 and in tables III, IV, and V. Coefficients are based on the area and/or chord of the wing alone. The data for the plain wing were obtained with the 20 percent chord flap fully retracted into its well. (See table II.) It is evident that an airplane having a flap of this type would have a much larger range of center-of-pressure travel between various flying conditions than would one with a plain wing. It appears, then, that in a normal type of 2-spar wing the effect of adding a Fowler flap would

be to leave the front-spar design load the same as for the wing without a flap but to increase considerably the

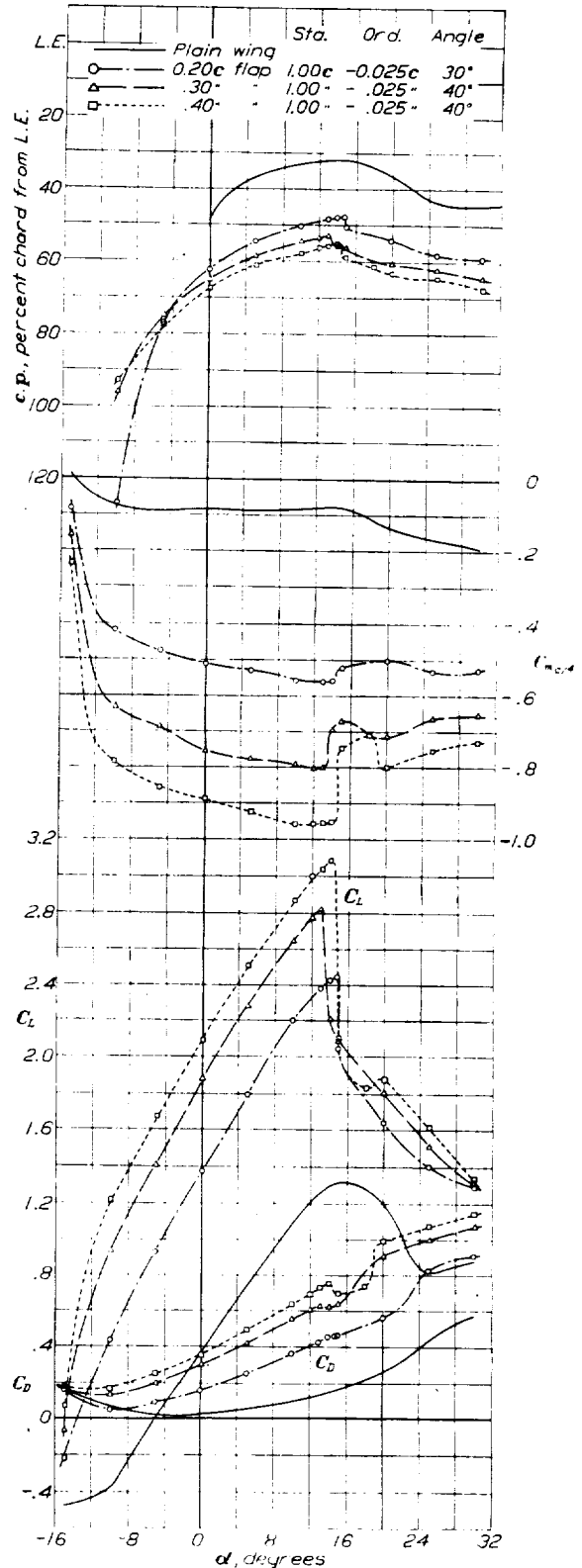


FIGURE 6.—Lift, drag, and pitching-moment coefficients for the maximum-lift condition.

design loads on the rear spar. If the speed at which the airplane may be flown with flap extended be limited to a value reasonably in excess of its landing speed, it appears likely that the loads with flap extended would be reduced to the same magnitude as the largest loads with flap retracted, with flap sizes not in excess of 30 percent  $c$ . On this basis it appears that a wing with a Fowler flap as wide as 30 percent  $c$  could be constructed in which there would be no increase in the weight of the wing structure proper, the only additional weight being due to the flap and its support from the spars.

**Take-off condition.**—Investigation of wing-flap combinations to determine the flap arrangement most favorable for take-off must involve consideration of performance parameters of the airplane in question as well as of the aerodynamic effects of the lifting surfaces. Concurrently with the tests, a series of take-off computations was made with the purpose of developing a "take-off criterion" for wings based on aerodynamic characteristics and depending on airplane design factors to the minimum extent possible. The application of such a criterion to the data would then serve to isolate the optimum flap arrangement for take-off. The development of the criterion, and associated data, are presented in an appendix to this report.

As the tests and computations progressed, it was found that some general considerations would serve to isolate the optimum arrangement, without recourse to a rigorous criterion. The computations indicated that normal transport airplanes should take off at a lift coefficient greater than 70 percent of the maximum available to achieve the shortest run to clear an obstacle. They also indicated that the principal aerodynamic characteristics affecting take-off, high lift available, and high  $L/D$  at the high lift are of nearly equal importance.

The wind-tunnel data, plotted as polar curves, are presented in figures 7 to 10 for the 0.30  $c$  flap and in figures 11 to 15 for the 0.20  $c$  flap. Comparison of these curves on the basis of the considerations previously stated indicated the flap position 0.025  $c$  directly below the trailing edge of the wing, with an angle of 30°, to be the optimum take-off arrangement for both flaps. At this setting each flap has as high ratios of  $L/D$  throughout the high-lift region as any other setting tested, within the limits of accuracy of the tests, and has a higher maximum lift coefficient than any other setting having as high ratios of  $L/D$ . The 40° setting of the 0.30  $c$  flap, at this same position, gives a higher maximum lift and lower ratio of  $L/D$  than the 30° angle, the percentage difference in  $L/D$  being greater than that in maximum lift. Computations (see appendix) verify the conclusion based on the general considerations, that the 30° angle is better with this flap.

Lift, drag, and pitching-moment data for the wing with each of three sizes of flap, with the flap at the

optimum setting for take-off, are given in figure 16 and in tables III, VI, and VII. The choice of the position 0.025  $c$  below the wing trailing edge, with a 25° angle, as optimum for the 40 percent  $c$  flap is based on the relation between optimum take-off setting and that for maximum lift of the 20 percent  $c$  and 30 percent  $c$  flaps. Although data for the 40 percent  $c$  flap are not sufficient for a rigorous selection, comparisons of data that are available (reference 2) indicate the choice to be sufficiently near the optimum for practical purposes.

**Partial retraction of flap.**—Lift, drag, and pitching-moment data for the wing with the 20 percent  $c$ , 30 percent  $c$ , and 40 percent  $c$  flaps in a partially retracted position are shown in figure 17 and in tables VIII to XI. The settings were chosen by assuming the flaps to move along an arc from the setting for maximum lift or optimum take-off to the fully retracted position. The flap hinges crossed the wing chord line at the 90 percent  $c$  station, and the angles at this position were 15° for the 20 percent  $c$  flap, 20° for the 30 percent  $c$  flap, and 20° and 30° for the 40 percent  $c$  flap. Comparison of the characteristics at this setting with those at the maximum-lift setting shows that the change of characteristics is in the same direction and of the same order of magnitude as the change of flap setting.

**Flap loads.**—Curves of normal- and longitudinal-force coefficients, hinge moments, and center-of-pressure locations of the 20 percent  $c$ , 30 percent  $c$ , and 40 percent  $c$  flaps in the maximum lift, optimum take-off, and partly retracted settings are shown in figures 18 to 23. The corresponding data appear in tables III to XI. From the magnitude of the load carried by the flap at high lift coefficients of the combination, it is evident that the flap carries nearly 1½ times its proportionate share of the total load. It appears that this type of flap may be regarded as a separate wing, operating in an air stream whose combined velocity and curvature increase considerably the load it carries as compared with the load it would experience in the free air stream. Comparison of load data for a split flap (reference 4) and a Fowler flap clearly shows the fundamental difference in the action of the two flaps. At high lifts, the split flap carries almost no lift and offers large drag; whereas the Fowler carries a large proportion of the total lift, but with less drag.

Although this condition is favorable to airplane performance, it implies a large range of center-of-pressure positions for the complete flight range, with consequent disadvantages in longitudinal-stability characteristics and possibly also in structure. In connection with structural considerations it is interesting to note that a progressive reduction in flap loads occurs with increasing flap size if the maximum angle is kept below 30°.

At flap settings giving high maximum lift coefficients, the center of pressure of the flap itself has little travel

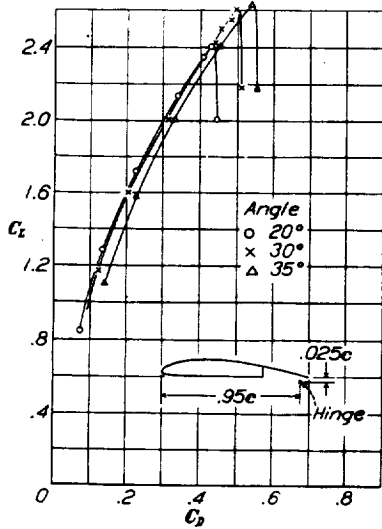


FIGURE 7.—Polars for 0.30 c flap at various angles.

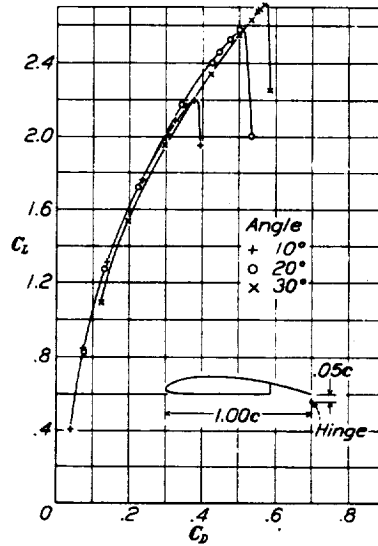


FIGURE 10.—Polars for 0.30 c flap at various angles.

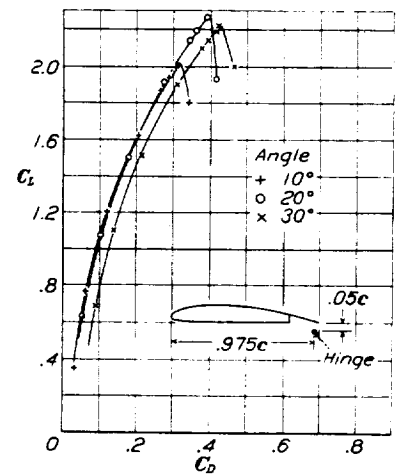


FIGURE 13.—Polars for 0.20 c flap at various angles.

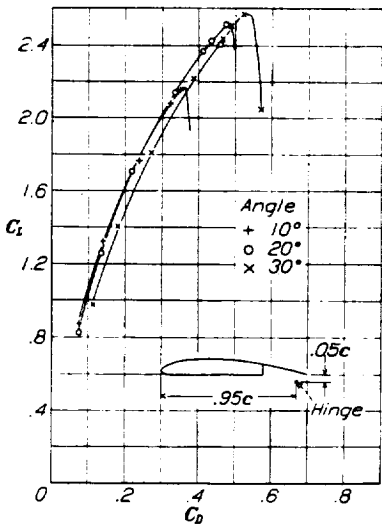


FIGURE 8.—Polars for 0.30 c flap at various angles.

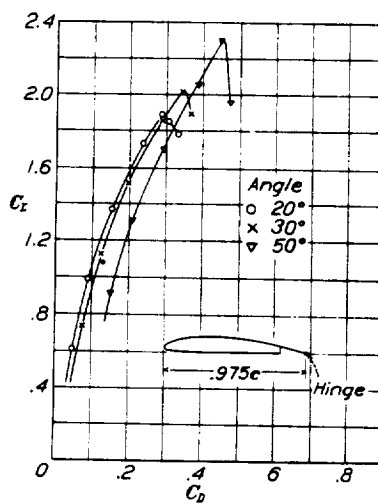


FIGURE 11.—Polars for 0.20 c flap at various angles.

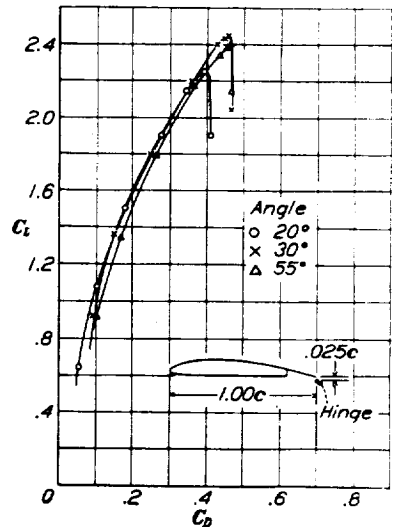


FIGURE 14.—Polars for 0.20 c flap at various angles.

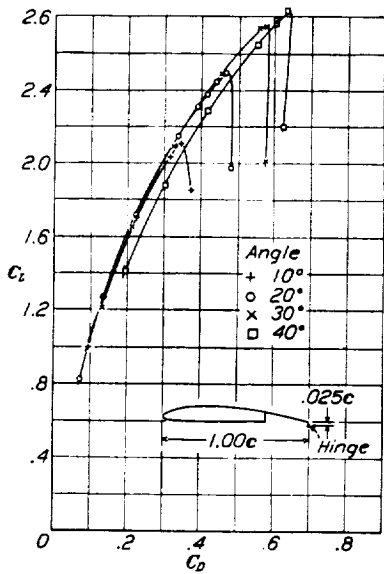


FIGURE 9.—Polars for 0.30 c flap at various angles.

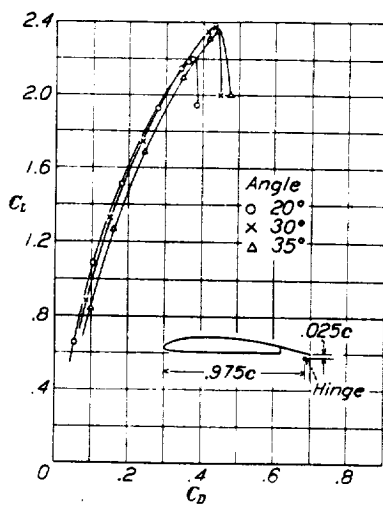


FIGURE 12.—Polars for 0.20 c flap at various angles.

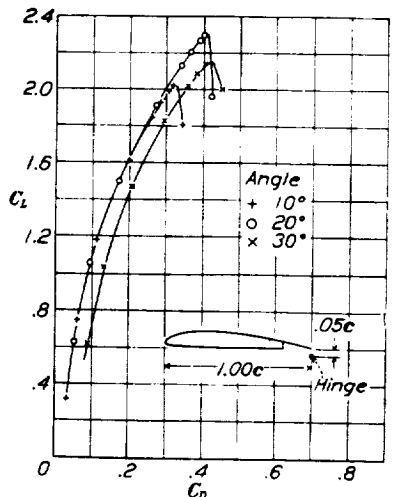


FIGURE 15.—Polars for 0.20 c flap at various angles.

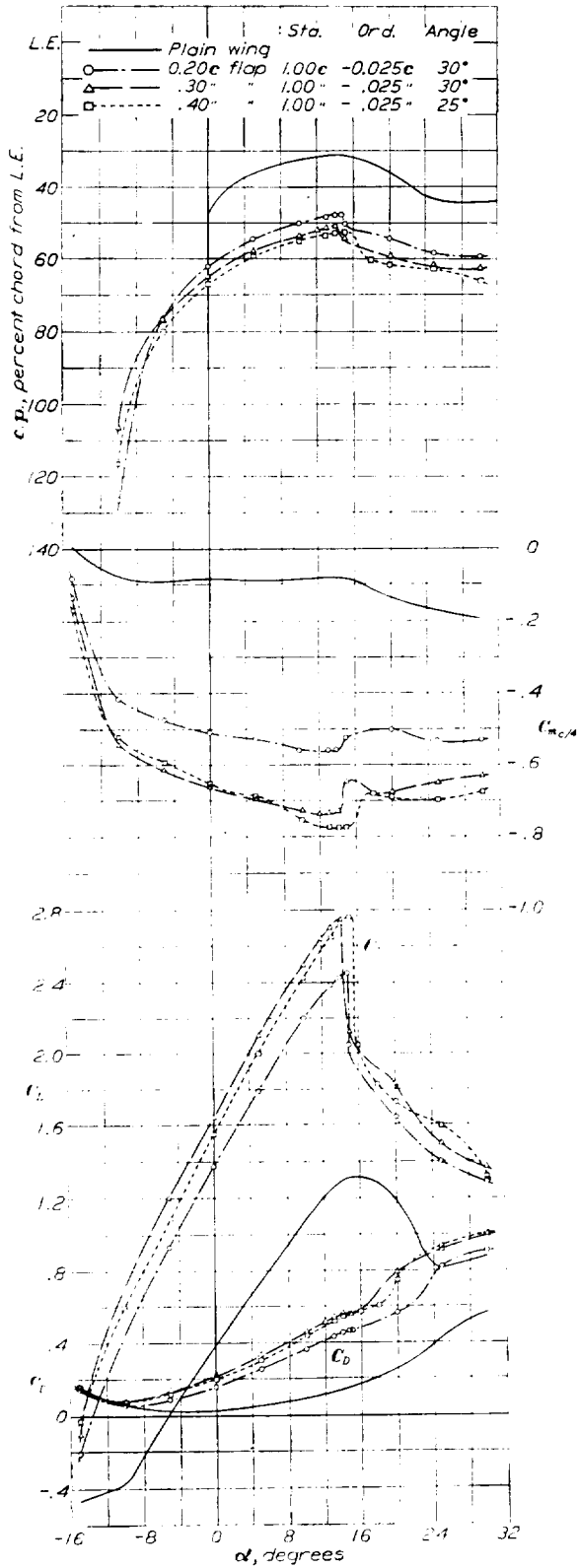


FIGURE 16.—Lift, drag, and pitching-moment coefficients for the optimum take-off condition.

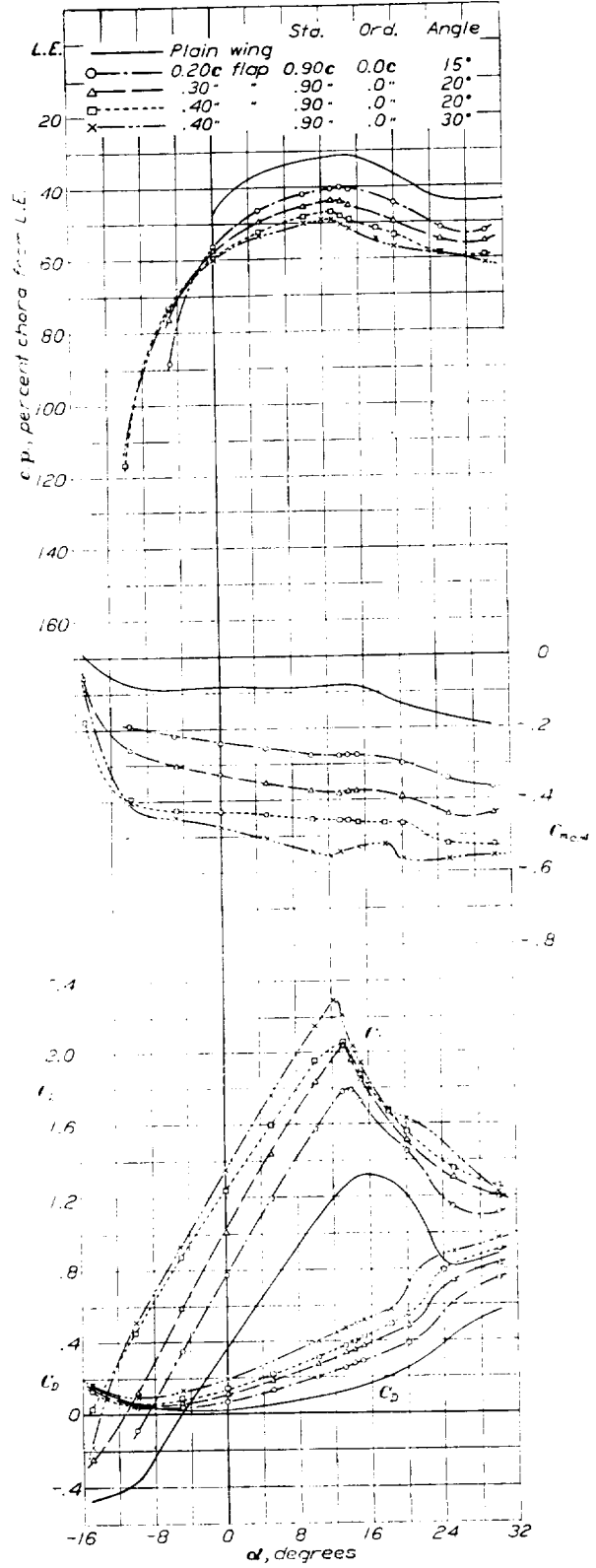


FIGURE 17.—Lift, drag, and pitching-moment coefficients for the partly retracted flap condition.

	Sta.	Ord.	Angle
o	0.20c flap	1.00c -0.025c	30°
Δ	.30" "	1.00" - .025"	40°
x	.40" "	1.00" - .025"	40°

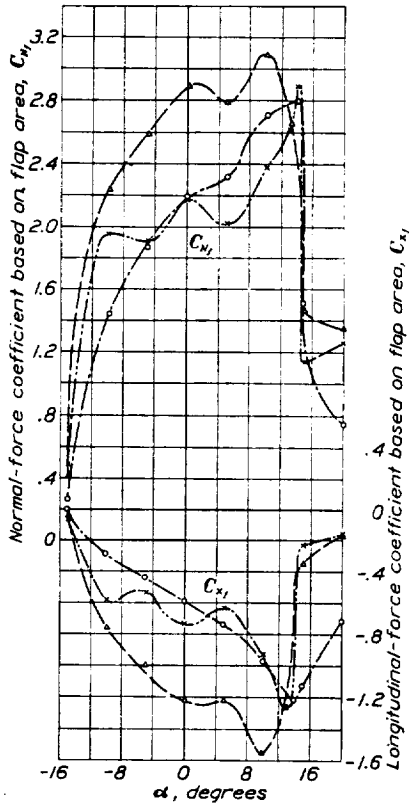


FIGURE 18.—Air loads on flaps for the maximum-lift condition.

	Sta.	Ord.	Angle
o	0.20c flap	1.00c -0.025c	30°
Δ	.30" "	1.00" - .025"	30°
x	.40" "	1.00" - .025"	25°

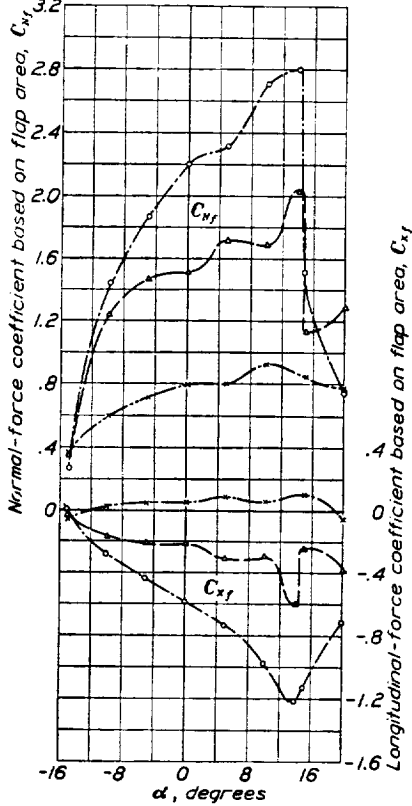


FIGURE 20.—Air loads on flaps for the optimum take-off condition.

	Sta.	Ord.	Angle
o	0.20c flap	0.90c 0.000c	15°
Δ	.30" "	.90" .000"	20°
□	.40" "	.90" .000"	20°
x	.40" "	.90" .000"	30°

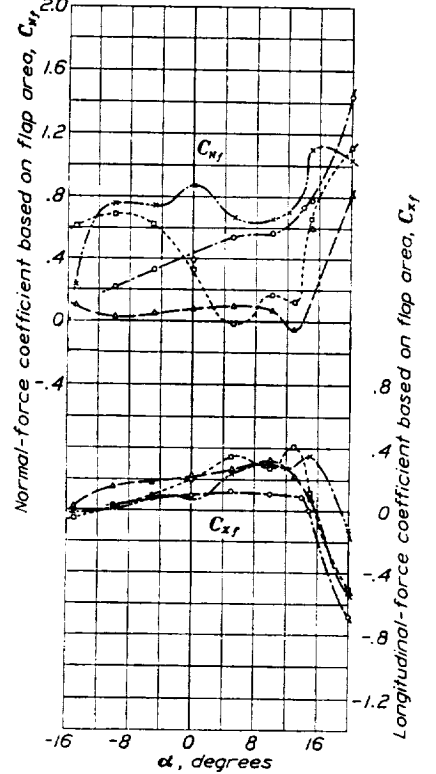


FIGURE 22.—Air loads on flaps for the partly retracted position.

	Sta.	Ord.	Angle
o	0.20c flap	1.00c -0.025c	30°
Δ	.30" "	1.00" - .025"	40°
x	.40" "	1.00" - .025"	40°

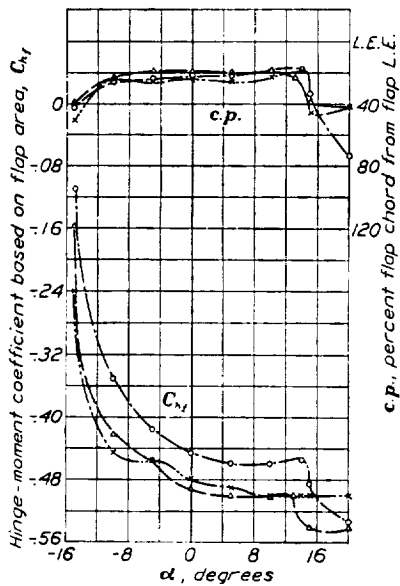


FIGURE 19.—Air moments on flaps for the maximum-lift condition.

	Sta.	Ord.	Angle
o	0.20c flap	1.00c -0.025c	30°
Δ	.30" "	1.00" - .025"	30°
x	.40" "	1.00" - .025"	25°

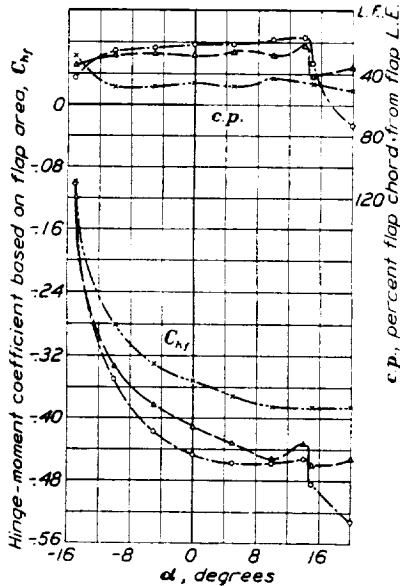


FIGURE 21.—Air moments on flaps for the optimum take-off condition.

	Sta.	Ord.	Angle
o	0.20c flap	0.90c 0.000c	15°
Δ	.30" "	.90" .000"	20°
□	.40" "	.90" .000"	20°
x	.40" "	.90" .000"	30°

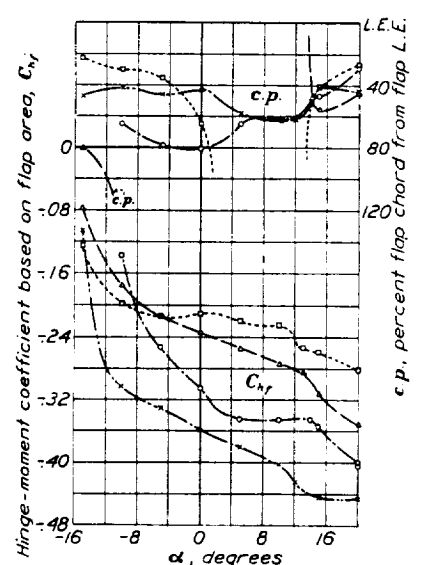


FIGURE 23.—Air moments on flaps for the partly retracted position.

throughout most of the angle-of-attack range and is generally nearer the leading edge than it would be on an airfoil in a free air stream. As the flap angle is reduced below 30°, however, the center of pressure moves rapidly backward.

**Downwash.**—Some representative data from the downwash measurements are shown in figures 24 and 25. Angle of downwash as a function of lift coefficient is shown for two positions behind the wing, with data for the plain wing and for the same flap settings as

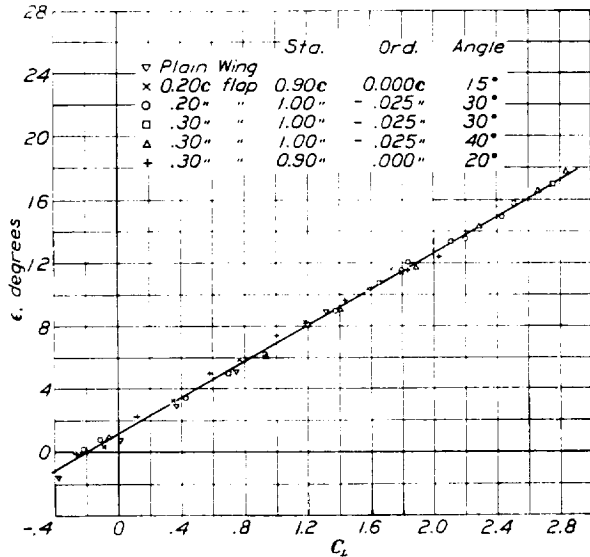


FIGURE 24.—Downwash angle against lift coefficient at a point behind the wing. Position of point: 2 c behind 0.25 chord point, 0.05 b laterally from center line, 0.5 c above wing chord.

were used in the flap load tests plotted on each curve. Only small consistent deviations from the mean curve, within the limits of test accuracy, were found for the variety of settings tested. It appears, then, that the addition of a Fowler flap has no appreciable effect on the basic relation between lift, span, and downwash at reasonable distances behind the wing.

The foregoing conclusion is subject to some question owing to the doubtful nature of the jet-boundary effect on downwash in the 7- by 10-foot tunnel. The corrections in this particular case differ considerably from the theoretical corrections, probably on account of the combined effect of static-pressure gradient in the jet and spillage of air over the unflared lip of the exit cone. Different corrections for different positions of the reference point in the air stream might produce greater consistent differences in downwash between the plain wing and flap extended conditions than are indicated by these tests, though this effect would be small unless the variation of the corrections with position is greater than seems likely.

Although the extensive investigation required to establish the corrections might produce results of academic interest, certain effects of combining a

variable-lift wing with an airplane fuselage would render the results of small technical value. Since a large difference in angle of attack occurs at the same value of  $C_L$  with different settings of the Fowler flap, a large variation of fuselage attitude and lift at a given wing lift coefficient results from changing flap settings. Thus, at a given over-all lift coefficient of the airplane, the lift coefficient and downwash of the wing may be expected to change with flap setting. The use of partial-span flaps produces an effective reduction of span as the flap is extended, causing an additional change of downwash at constant lift coefficient with changing flap setting. It appears that problems involving downwash of variable-lift wings are more susceptible of solution by measurement on

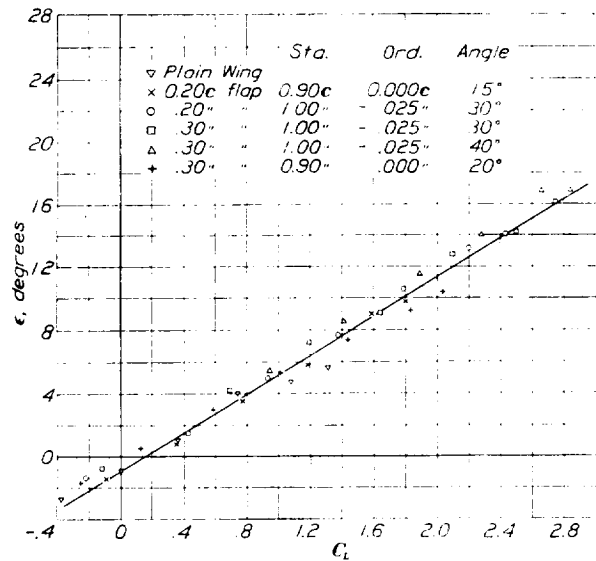


FIGURE 25.—Downwash angle against lift coefficient at a point behind the wing. Position of point: 3 c behind 0.25 chord point, 0.05 b laterally from center line, on chord line.

the actual design in question, rather than by a fundamental wind-tunnel investigation.

**CONCLUSIONS**

1. The maximum lift coefficients, based on area of wing alone, found for the three sizes of flap tested were: For the 20 percent  $c$  flap, 2.45; for the 30 percent  $c$  flap, 2.85; and for the 40 percent  $c$  flap, 3.17. The maximum lift coefficient for the wing with flap retracted was 1.31.

2. The location of the flap leading edge for maximum lift was found to be the same in all cases, the center of the leading-edge arc being 2.5 percent  $c$  directly below the trailing edge of the main wing. The flap angles for maximum lift were 30°, 40°, and 40° for the 20 percent  $c$ , 30 percent  $c$ , and 40 percent  $c$  flaps, respectively.

3. The 20 percent  $c$  and 30 percent  $c$  flaps were found to give the characteristics most favorable to

take-off with the same leading-edge location as for maximum lift. The optimum angle was  $30^\circ$  in both cases.

4. The maximum normal-force and longitudinal-force coefficients of the 40 percent  $c$  flap, based on flap area, were 2.89 and  $-1.25$ ; those for the 30 percent  $c$  flap were 3.06 and  $-1.54$ ; and those for the 20 percent  $c$  flap were 2.80 and  $-1.20$ . Center-of-pressure locations corresponding to these coefficients were in each case approximately at the 20 percent  $c$  flap chord points.

5. At positions normally occupied by the tail surfaces the relation between lift coefficient and downwash angle appears from the present tests to be the same for a wing with or without a full-span Fowler flap.

LANGLEY MEMORIAL AERONAUTICAL LABORATORY,  
NATIONAL ADVISORY COMMITTEE FOR AERONAUTICS,  
LANGLEY FIELD, VA., *April 26, 1935.*

## APPENDIX

### TAKE-OFF

The computations leading to the results presented here were made concurrently with a more detailed set of computations of the effect of various types of flap on take-off, reported in reference 6. Only a brief résumé of the assumptions made and of the equations used is given here, since they are identical except in two minor respects with those of the foregoing reference.

**Assumptions.**—The airplane is assumed to take off in a calm, from a surface having a friction coefficient of 0.05, and to maintain constant air speed after leaving the ground until it clears an obstacle at an altitude of 50 feet. Further assumptions are that the airplane has a constant parasite-drag coefficient (excluding wing drag completely) of 0.023 over the full angle-of-attack range and is equipped with an automatic propeller giving maximum efficiency at top speed. No allowance for induced drag at maximum speed is made.

It is considered reasonable to neglect factors that would be assumed to be the same in comparable cases. On this basis the effects of wind, wind-velocity gradient with height, proximity of the ground, and slipstream over parts of the wing are excluded from the computations. In the estimation of the effect of flaps this assumption is conservative since wind, ground effect, and slipstream are all more helpful to high-lift devices than to normal wings, and wind-velocity gradient is more helpful to the normal wing.

The only differences between the assumptions used here and those of reference 6 are in the parasite-drag coefficient and in the attitude during ground run. For the other computations the parasite coefficient was 0.020 and the attitude giving minimum total resistance during ground run was used. This assumption required a negative angle of attack of the Fowler wing, an attitude that is not feasible during the ground run because of danger of nosing over or of damaging the propeller. An angle of attack of 0° during the ground run was used in the computations for the present report.

**Equations.**—In order that the equations may correctly represent the processes occurring during the take-off of an airplane over an obstacle, it is necessary to consider the take-off as divided into three phases: ground run—a period of horizontal acceleration with the weight partly wheelborne and partly airborne; transition—a period of vertical acceleration to a steady rate of climb; and the steady climb from the height reached in transition to the height of the obstacle.

Subject to the limitations previously stated, the horizontal distance covered during each of the phases may be computed from the following equations.

Ground run, feet:

$$D_1 = \frac{W/S}{\rho g (\mu C_{L_1} - C_{D_1} - B \frac{W/S}{W/hp.})} \times \log_e \left[ 1 + \frac{\mu C_{L_1} - C_{D_1} - B \frac{W/S}{W/hp.}}{\left( \frac{A}{W/hp.} - \mu \right) C_{L_T}} \right]$$

Transition, feet:

$$D_2 = \frac{2W/S}{\rho g} \left( \frac{1}{C_{L_{max}} - C_{L_T}} \right) \sin \theta$$

Steady climb, feet:

$$D_3 = \frac{H_2 \frac{2W/S}{\rho g} \left( \frac{1}{C_{L_{max}} - C_{L_T}} \right) (1 - \cos \theta)}{\tan \theta}$$

The angle of climb  $\theta$  appearing in the last two phases is found from the relation:

$$\sin \theta = \frac{A}{W/hp.} - \left( B \frac{W/S}{W/hp.} + C_{D_T} \right) \frac{1}{C_{L_T}}$$

The symbols appearing in the foregoing equations are defined as follows:

- $\rho$ , air density, slugs per cu. ft.
- $g$ , acceleration of gravity, ft./sec.<sup>2</sup>
- $\mu$ , ground friction coefficient, assumed equal to 0.05.

$W/S$ , wing loading, lb. per sq. ft.

$W/hp.$ , power loading, lb. per h. hp.

$C_{L_1}$ ,  $C_{D_1}$ , lift and drag coefficients at angle of attack maintained during ground run.

$C_{L_T}$ ,  $C_{D_T}$ , lift and drag coefficients corresponding to  $V_T$ , the speed at which the airplane leaves the ground. It is to be noted that the airplane must fly at a higher lift coefficient than  $C_{L_T}$  during transition, since the flight path is curved upward and the speed remains equal to  $V_T$ .

$A$ ,  $B$ , constants expressing thrust of an automatic propeller at low forward speeds. Thrust = b. hp. ( $A - B \rho/2 V^2$ ). The constants apply to any one airplane, and vary with top speed among various airplanes.

$H_2$ , height of obstacle, assumed 50 feet.

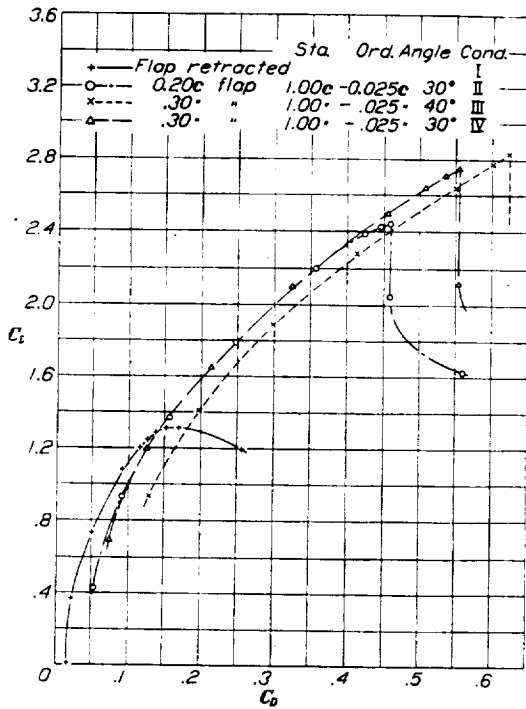


FIGURE 26.—Polars for take-off computations. The value of  $C_D$  does not include the airplane parasite-drag coefficient.

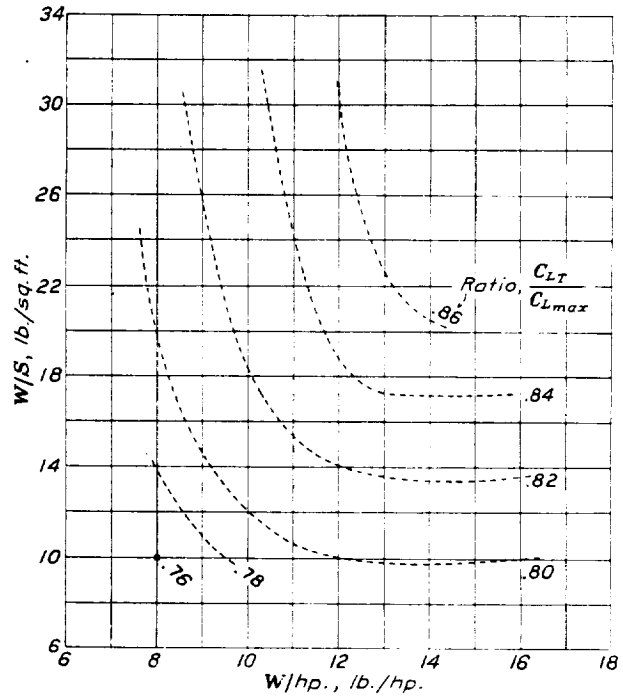


FIGURE 28.— $C_{LT}/C_{Lmax}$  for minimum take-off run as a function of wing and power loading.

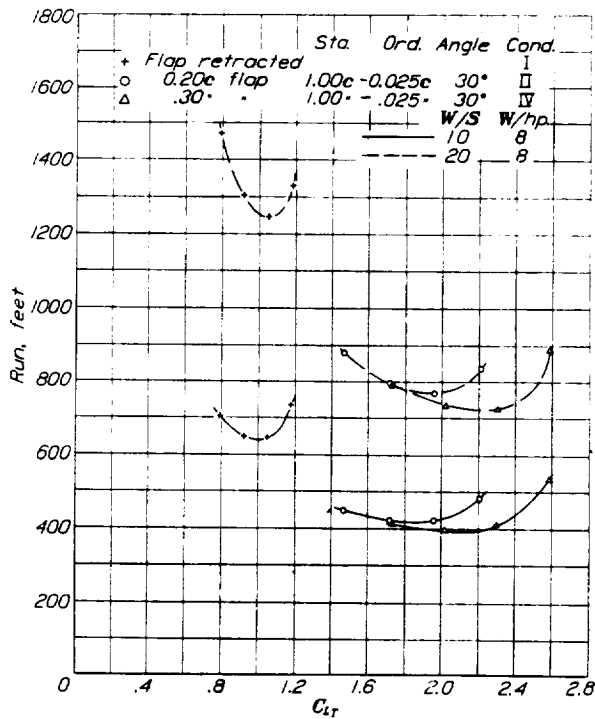


FIGURE 27.—Take-off run against lift coefficient.

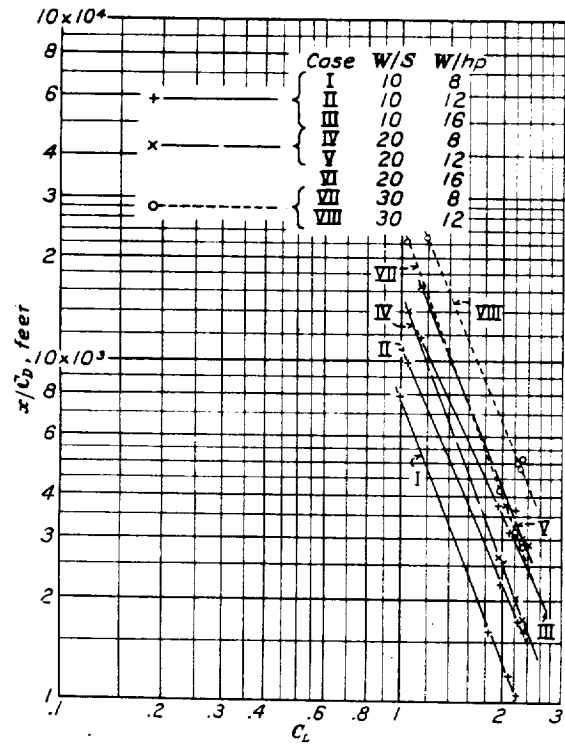


FIGURE 29.—Take-off run as a function of  $C_L$  and  $C_D$ .

The computations covered a range of wing loading between 10 pounds per square foot and 30 pounds per square foot and a range of power loading between 8 pounds per horsepower and 16 pounds per horsepower. Eight combinations of wing and power loading, designated "cases" and listed in table XII, together with the corresponding airplane and propeller characteristics, were considered. In combination with the eight cases, four wing conditions were taken as follows:

- I. Plain wing; flap retracted.
- II. 20 percent  $c$  flap; station, 100 percent  $c$ ; ordinate,  $-2.5$  percent  $c$ ; angle,  $30^\circ$ .
- III. 30 percent  $c$  flap; station, 100 percent  $c$ ; ordinate,  $-2.5$  percent  $c$ ; angle,  $40^\circ$ .
- IV. 30 percent  $c$  flap; station and ordinate, same as for III; angle,  $30^\circ$ .

Polar curves for the wing in the various conditions, from the wind-tunnel data, are shown in figure 26. For each combination of airplane case and wing condition, the take-off runs at four values of  $V_T$ , corresponding to lift coefficients of 60 percent, 70 percent, 80 percent, and 90 percent of  $C_{L_{max}}$  for the wing condition in question, were computed. The results, showing total run required by the hypothetical airplane to reach an altitude of 50 feet in a steady climb from a standing start with no wind, are presented in table XIII. Table XIV shows corresponding values of the ground run alone. This table is included for use in cases where the ground run alone, rather than the take-off over an obstacle, is the factor to be considered. The results are satisfactory for comparison among themselves but should not be relied upon as being accurate in an actual case. They are probably conservative for an airplane with an automatic propeller taking off from an average field with no wind.

Representative curves of total take-off run against take-off lift coefficient ( $C_{L_T}$ ) for several cases and conditions are shown in figure 27. All the data of table XIII were plotted in similar fashion and the optimum value of  $C_{L_T}$  was found for each case and condition. The optimum ratio of  $C_{L_T}/C_{L_{max}}$  was nearly constant for the various wing and flap conditions at a given wing and power loading but varied with wing and power loading. Figure 28 shows the optimum value of  $C_{L_T}/C_{L_{max}}$  as a function of wing and power loading for the range covered in the computations.

Consideration of the analysis at this point indicated that it might be possible to develop a general relation between lift and drag which would give correct weight to these two factors in take-off, independently of other factors. It appears that a ratio  $C_L^n/C_D$  would place extra weight on lift in accordance with its extra importance if a satisfactory value for  $n$  could be determined. For each of the eight cases, the minimum take-off run and the corresponding  $C_L$  and  $C_D$  for each condition were plotted as in figure 29. When

the minimum take-off run  $x$  was divided by the corresponding  $C_D$  and plotted against  $C_L$  on logarithmic paper, the data for any case lay very nearly in a straight line. The form of the equation for this function is  $\frac{x}{C_D} = K C_L^n$  and, if  $K$  and  $n$  be expressed as functions of wing and power loading, a general take-off equation in very simple form is obtained. It will be noted in figure 29 that  $n$  is nearly constant over the range of cases considered and that the average value of  $n$  is  $-2.4$ ; that is,  $\frac{x}{C_D} = K C_L^{-2.4}$ , which may be reduced to the form  $K/x = C_L^{-2.4}/C_D$ . This ratio may be considered a "take-off criterion", the value of total take-off distance of an airplane being inversely proportional to the value of  $C_{L_T}^{2.4}/C_{D_T}$  for its wing at the ratio of  $C_{L_T}/C_{L_{max}}$  in question.

It will be noted that the curve for case VI, having a wing loading of 20 and a power loading of 16, is not included in figure 29. The data are not directly applicable in this case because the power available is seriously inadequate to satisfy the assumption that the airplane fly through the transition at its maximum lift coefficient without loss of speed. Thus, the computed runs are incorrect even assuming the runs in other cases to be strictly correct as computed.

When using the criterion, it is first necessary to select the ratio of  $C_{L_T}/C_{L_{max}}$  for minimum run from figure 28, depending on the approximate wing and power loading of the design in hand. Then in order to compare the take-off properties of different wing and flap combinations it is necessary to compare the values of the criterion  $C_{L_T}^{2.4}/C_{D_T}$  where  $C_{L_T}$  for any power loading is shown plotted on semilogarithmic paper in figures 30, 31, 32, and 33 for each of the four wing-flap combination is the optimum fraction of the  $C_{L_{max}}$  of that combination (obtained from fig. 28) and  $C_{D_T}$  is the corresponding drag coefficient of the combination. The criterion should give satisfactory comparison between normal airfoils with or without high-lift devices. Some comparisons of cases selected from reference 6 have shown that the criterion gives a good indication of the relative merits of the various devices considered in take-off, although when used for other devices than the Fowler flap the values of the criterion are not inversely proportional to the take-off runs within as close limits.

Development of the criterion was based on measured  $C_D$  of the wing only, to permit comparison of various wings as tested in the wind tunnel without a body. Variations in parasite drag of the rest of the airplane will have small effect since the wing drag is a large portion of the total drag at any lift coefficient near  $C_{L_{max}}$ , particularly with high-lift devices.

The variation of total take-off run with wing and

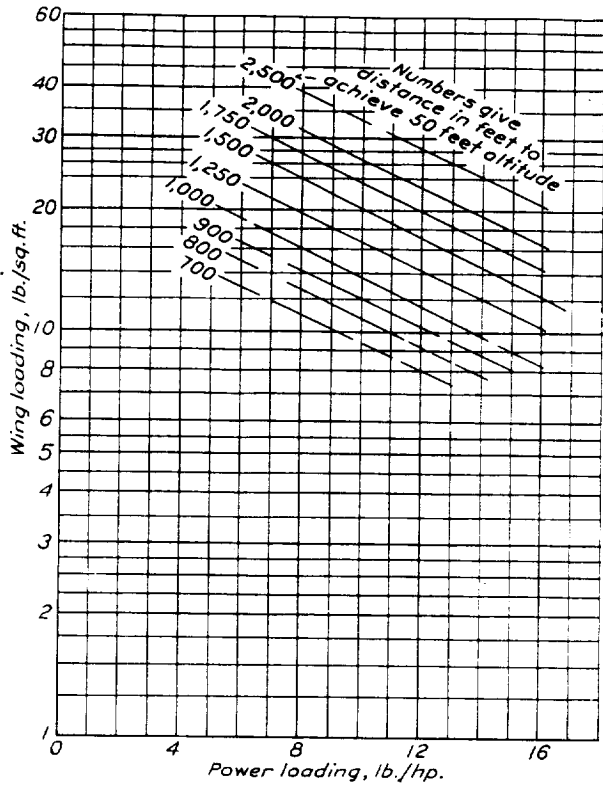


FIGURE 30.—Minimum take-off run with various power and wing loadings. Condition I, flap retracted.

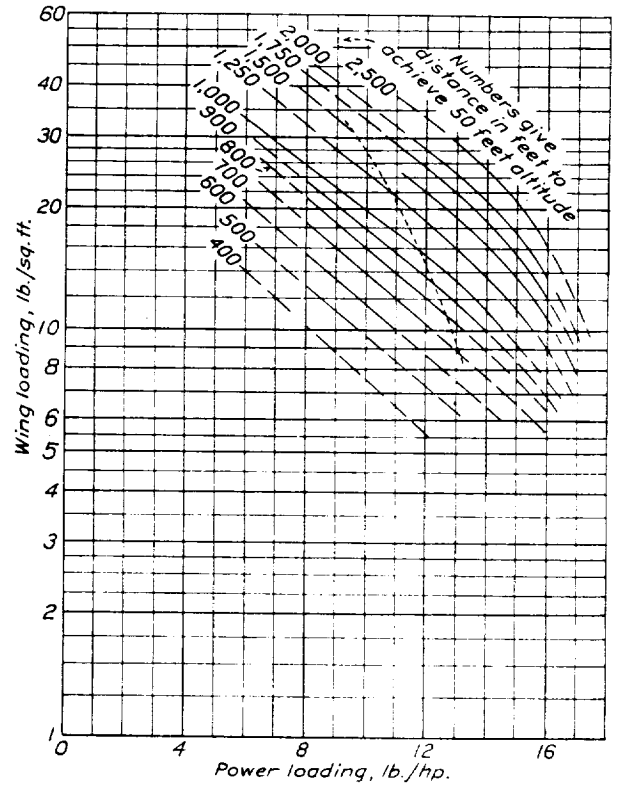


FIGURE 32.—Minimum take-off run with various power and wing loadings. Condition III, 0.30 c flap; flap station, 1.00 c; ordinate, -0.025 c; angle, 40°.

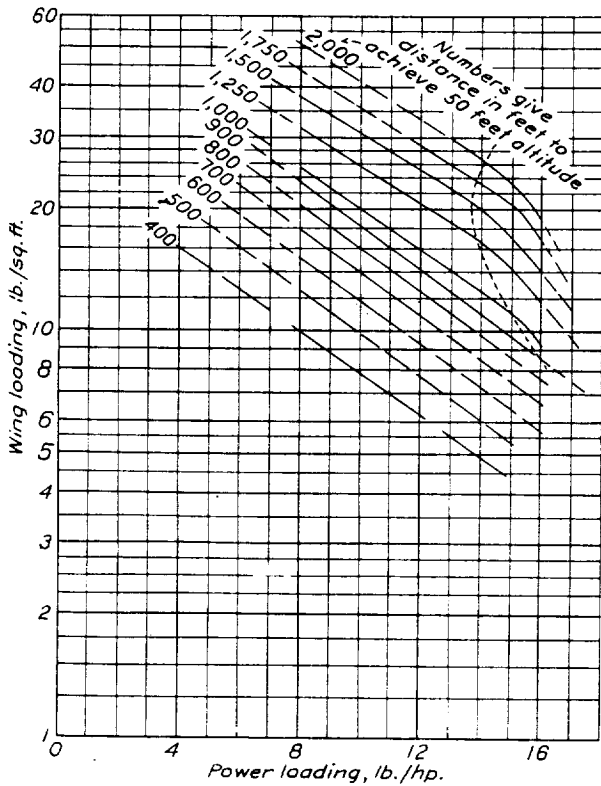


FIGURE 31.—Minimum take-off run with various power and wing loadings. Condition II, 0.20 c flap; flap station, 1.00 c; ordinate, -0.025 c; angle, 30°.

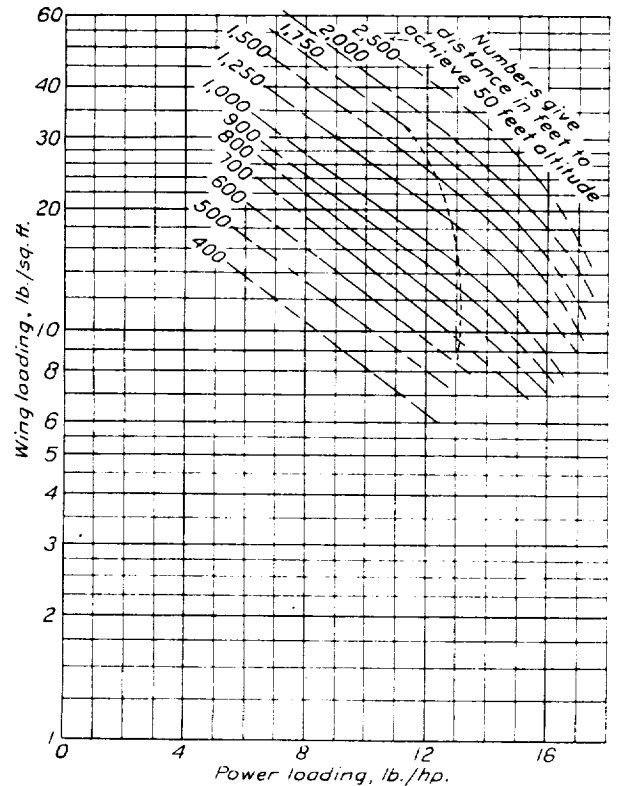


FIGURE 33.—Minimum take-off run with various power and wing loadings. Condition IV, 0.30 c flap; flap station, 1.00 c; ordinate, -0.025 c; angle, 30°.

wing conditions. In the last three figures a portion of the lines at the high power loadings is curved. This curvature appears to lie within the region indicated by a dotted line, which shows the combined power and wing loading at which the power available is insufficient to satisfy the transition assumption at the instant of leaving the ground. No correction has been made for this effect, but in table XIII an approximate correction is noted opposite the points to which it applies. In the range covered, the error appears sufficiently small to be neglected for practical purposes.

Although figures 30 to 33 are accurate only for determining the relative take-off runs of airplanes with various wing and power loadings and arrangements of the Fowler flap, it is believed that they may be applied within reasonable limits to actual cases. Assuming good piloting technique, and using an automatic propeller, the data represent the minimum run that an airplane might be expected to need to clear a 50-foot obstacle with a reasonable margin of speed. It is to be noted that the foregoing statement applies to cases in which the ground is at least as smooth and hard as the average airport.

The computations appear, in general, to justify the conclusion that, within the normal range of wing and power loadings, a wing with a Fowler flap can produce considerable improvement in take-off as compared with a plain wing.

REFERENCES

1. Fowler, Harlan D.: Variable Lift. Western Flying, Nov. 1931, pp. 31-33.
2. Weick, Fred E., and Platt, Robert C.: Wind-Tunnel Tests of the Fowler Variable-Area Wing. T. N. No. 419, N. A. C. A., 1932.
3. Harris, Thomas A.: The 7- by 10-Foot Wind Tunnel of the National Advisory Committee for Aeronautics. T. R. No. 412, N. A. C. A., 1931.
4. Wenzinger, Carl J.: Wind-Tunnel Measurements of Air Loads on Split Flaps. T. N. No. 498, N. A. C. A., 1934.
5. Theodorsen, Theodore, and Silverstein, Abe: Experimental Verification of the Theory of Wind-Tunnel Boundary Interference. T. R. No. 478, N. A. C. A., 1934.
6. Wetmore, J. W.: Calculated Effect of Various Types of Flap on Take-Off over Obstacles. (To be published at later date.)

TABLE I  
AIRFOIL ORDINATES  
CLARK Y

(All values in percent airfoil chord)

Station	Ordinate upper	Ordinate lower	Station	Ordinate upper	Ordinate lower
0	3.50	3.50	40	11.40	0
1.25	5.45	1.93	50	10.52	0
2.50	6.50	1.47	60	9.15	0
3.75	7.90	.93	70	7.35	0
5.00	8.85	.43	80	5.22	0
7.50	9.60	.42	90	2.80	0
10	10.68	.15	95	1.49	0
15	11.36	.03	100	.12	0
20	11.70	0			
30					

Leading-edge radius=1.50.

TABLE II  
PLAIN WING  
(Flap retracted)

$\alpha$	$C_L$	$C_D$	$C_{m_{c/4}}$
Degrees			
-15	-0.480	0.168	0.011
-10	-.383	.039	-.071
-5	-.005	.017	-.089
-4	.080	.015	.....
0	.365	.023	-.085
5	.735	.050	-.084
10	1.080	.092	-.085
12	1.200	.116	-.081
13	1.246	.127	-.080
14	1.288	.138	-.082
15	1.310	.152	-.082
16	1.310	.170	.....
17	1.300	.191	.....
20	1.195	.256	-.133
25	.815	.433	-.170
30	.375	.568	-.197

TABLE III  
DATA FOR THE MAXIMUM-LIFT CONDITION  
(0.20c flap; flap station, 1.00c; ordinate, -0.025c; angle, 30°)

$\alpha$	$C_L$	$C_D$	$C_{m_{c/4}}$	$C_{N_f}$	$C_{x_f}$	$C_{y_f}$
Degrees						
-15	-0.222	0.159	-0.092	0.296	0.005	-0.109
-10	-.427	.053	-.417	1.441	-.280	-.350
-5	.926	.091	-.472	1.875	-.430	-.417
0	1.370	.157	-.508	2.500	-.590	-.417
5	1.790	.247	-.527	2.324	-.735	-.459
10	2.200	.359	-.555	2.715	-.975	-.458
13	2.385	.424	-.558	.....	.....	.....
14	2.431	.447	-.556	2.800	-1.210	-.453
14.5	2.445	.459	-.548	.....	.....	.....
15	2.045	.480	-.522	1.513	-1.115	-.484
20	1.645	.561	-.500	.7435	-7.15	-.532
25	1.400	.820	-.531	.....	.....	.....
30	1.287	.905	-.529	.....	.....	.....

TABLE IV  
DATA FOR THE MAXIMUM-LIFT CONDITION  
(0.30c flap; flap station, 1.00c; ordinate, -0.025c; angle, 40°)

$\alpha$	$C_L$	$C_D$	$C_{m_{c/4}}$	$C_{N_f}$	$C_{x_f}$	$C_{y_f}$
Degrees						
-15	-0.067	0.172	-0.155	0.420	-0.03	-0.157
-10	.931	.128	-.633	2.253	-.76	-.422
-5	1.403	.196	-.689	2.594	-.99	-.452
0	1.882	.300	-.754	2.889	-1.22	-.491
5	2.290	.413	-.775	2.791	-1.21	-.501
10	2.650	.550	-.793	3.085	-1.54	-.511
12	2.780	.601	-.806	.....	.....	.....
13	2.827	.624	-.801	2.665	-1.25	-.501
14	2.205	.618	-.696	.....	.....	.....
15	2.163	.638	-.676	1.466	-.35	-.510
20	1.805	.907	-.713	1.355	-.16	-.540
25	1.510	.996	-.684	.....	.....	.....
30	1.300	1.065	-.655	.....	.....	.....

TABLE V  
DATA FOR THE MAXIMUM-LIFT CONDITION  
(0.40c flap; flap station, 1.00c; ordinate, -0.025c; angle, 40°)

$\alpha$	$C_L$	$C_D$	$C_{m_{c/4}}$	$C_{N_f}$	$C_{x_f}$	$C_{y_f}$
Degrees						
-15	0.064	0.175	-0.236	0.485	-0.060	-0.239
-10	1.209	.165	-.785	1.950	-.580	-.445
-5	1.673	.251	-.856	1.908	-.528	-.456
0	2.095	.358	-.886	2.168	-.730	-.478
5	2.510	.489	-.923	2.020	-.630	-.489
10	2.875	.636	-.958	2.375	-.928	-.499
12	3.005	.690	-.955	.....	.....	.....
13	3.040	.727	-.956	2.620	-1.250	.....
14	3.095	.742	-.953	2.890	.....	-.499
15	2.100	.690	-.749	1.133	-.228	-.499
18	1.825	.735	-.711	.....	.....	.....
20	1.885	.985	-.803	1.255	-.155	-.449
25	1.613	1.071	-.784	.....	.....	.....
30	1.335	1.140	-.732	.....	.....	.....

TABLE VI  
DATA FOR THE OPTIMUM TAKE-OFF CONDITION  
(0.30c flap; flap station, 1.00c; ordinate, -0.025c; angle, 30°)

$\alpha$	$C_L$	$C_D$	$C_{m_{dl}}$	$C_{N_f}$	$C_{X_f}$	$C_{h_f}$
Degrees						
-15.....	-0.118	0.152	-0.133	0.355	-0.04	-0.118
-10.....	.693	.075	-.543	1.241	-.17	-.334
-5.....	1.198	.131	-.611	1.464	-.21	-.383
0.....	1.645	.215	-.658	1.512	-.22	-.412
5.....	2.100	.325	-.696	1.716	-.31	-.432
10.....	2.500	.456	-.729	1.682	-.30	-.452
12.....	2.645	.508	-.733			
13.....	2.705	.536	-.732			
14.....	2.750	.555	-.728	2.033	-.60	-.432
15.....	2.115	.555	-.648	1.138	-.25	-.461
20.....	1.830	.787	-.678	1.292	-.38	-.452
25.....	1.800	.911	-.650			
30.....	1.366	1.000	-.631			

TABLE VII.—DATA FOR THE OPTIMUM TAKE-OFF CONDITION

(0.40c flap; flap station, 1.00c; ordinate, -0.025c; angle, 25°)

$\alpha$	$C_L$	$C_D$	$C_{m_{dl}}$	$C_{N_f}$	$C_{X_f}$	$C_{h_f}$
Degrees						
-15.....	-0.032	0.133	-0.168	0.368	-0.055	-0.099
-10.....	.587	.064	-.521	.600	-.030	-.282
-5.....	1.086	.113	-.592	.710	-.043	-.331
0.....	1.548	.193	-.650	.793	-.045	-.353
5.....	1.995	.299	-.699	.900	-.068	-.372
10.....	2.425	.428	-.752	.928	-.068	-.366
13.....	2.650	.518	-.774			
14.....	2.718	.545	-.775			
15.....	2.760	.569	-.774	.848	.106	-.386
16.....	2.045	.568	-.680			
18.....	1.825	.801	-.690			
20.....	1.730	.745	-.699	.780	-.050	-.386
25.....	1.595	.931	-.677			
30.....	1.315	1.000				

TABLE VIII.—DATA FOR THE PARTLY RETRACTED CONDITION

(0.20c flap; flap station, 0.90c; ordinate, 0.0c; angle, 15°)

$\alpha$	$C_L$	$C_D$	$C_{m_{dl}}$	$C_{N_f}$	$C_{X_f}$	$C_{h_f}$
Degrees						
-10.....	-0.088	0.035	-0.187	0.219	0.040	-0.139
-5.....	.347	.036	-.218	.329	.080	-.254
0.....	.770	.065	-.239	.387	.095	-.306
5.....	1.182	.121	-.253	.538	.115	-.344
10.....	1.630	.196	-.271	.561	.115	-.344
12.....	1.772	.246	-.274			
14.....	1.795	.266	-.271	.738	.090	-.344
15.....	1.725	.285	-.272	.777	-.005	-.356
20.....	1.450	.392	-.295	1.438	-.685	-.406
25.....	1.135	.602	-.339			
30.....	1.110	.744	-.363			

TABLE IX.—DATA FOR THE PARTLY RETRACTED CONDITION

(0.30c flap; flap station, 0.90c; ordinate, 0.0c; angle 20°)

$\alpha$	$C_L$	$C_D$	$C_{m_{dl}}$	$C_{N_f}$	$C_{X_f}$	$C_{h_f}$
Degrees						
-15.....	-0.255	0.156	-0.055	0.100	0.080	-0.071
-10.....	.118	.064	-.257	.025	.157	-.177
-5.....	.580	.060	-.301	.049	.183	-.216
0.....	1.005	.106	-.327	.079	.237	-.236
5.....	1.430	.175	-.352	.095	.277	-.256
10.....	1.830	.268	-.376	.064	.337	-.275
13.....	2.028	.326	-.381	-.068	.227	-.285
14.....	1.955	.346	-.376			
15.....	1.842	.370	-.375	.598	.087	-.314
20.....	1.508	.480	-.390	.817	-.520	-.364
25.....	1.300	.780	-.442			
30.....	1.190	.821	-.439			

TABLE X  
DATA FOR THE PARTLY RETRACTED CONDITION

(0.40c flap; flap station, 0.90c; ordinate, 0.0c; angle, 20°)

$\alpha$	$C_L$	$C_D$	$C_{m_{dl}}$	$C_{N_f}$	$C_{X_f}$	$C_{h_f}$
Degrees						
-15.....	0.030	0.133	-0.174	0.610	-0.055	-0.127
-10.....	.445	.049	-.393	.688	.023	-.198
-5.....	.872	.082	-.427	.625	.090	-.215
0.....	1.231	.139	-.429	.328	.200	-.210
5.....	1.594	.214	-.438	-.015	.348	-.220
10.....	1.946	.304	-.452	.175	.275	-.226
13.....	2.054	.370	-.455	.123	.403	-.254
14.....	1.945	.368	-.456			
15.....	1.872	.428	-.462	.663	.113	-.259
18.....	1.675	.494	-.463			
20.....	1.555	.544	-.466	1.120	-.513	-.282
25.....	1.350	.795	-.522			
30.....	1.287	.907	-.524			

TABLE XI  
DATA FOR THE PARTLY RETRACTED CONDITION

(0.40c flap; flap station, 0.90c; ordinate, 0.0c; angle, 30°)

$\alpha$	$C_L$	$C_D$	$C_{m_{dl}}$	$C_{N_f}$	$C_{X_f}$	$C_{h_f}$
Degrees						
-15.....	-0.189	0.159	-0.088	0.230	-0.023	-0.105
-10.....	.502	.086	-.407	.753	.010	-.304
-5.....	.924	.128	-.446	.740	.082	-.331
0.....	1.342	.192	-.473	.868	.078	-.359
5.....	1.753	.284	-.505	.690	.235	-.381
10.....	2.145	.390	-.544	.653	.290	-.403
12.....	2.285	.445	-.556	.693	.268	-.425
13.....	2.210	.469	-.543			
14.....	2.025	.492	-.534			
15.....	1.930	.515	-.531	1.100	.350	-.445
18.....	1.690	.576	-.523			
20.....	1.630	.724	-.564	1.038	-.125	-.447
25.....	1.440	.895	-.566			
30.....	1.220	.969	-.557			

TABLE XII  
AIRPLANE CHARACTERISTICS FOR TAKE-OFF COMPUTATIONS

Case	Wing loading, W/S	Power loading, W/hp.	$C_{D_{min}}$	Maximum speed	A	B
I	lb./sq. ft.	lb./hp.		m. p. h.		
II	10	12	0.033	180	3.90	0.067
III	10	14	.033	123	4.18	.083
IV	20	8	.033	200	3.34	.082
V	20	12	.033	177	3.69	.082
VI	20	16	.033	161	3.89	.066
VII	30	8	.033	230	2.79	.012
VIII	30	12	.033	195	3.41	.037

TABLE XIII  
COMPUTED TAKE-OFF RUNS IN FEET

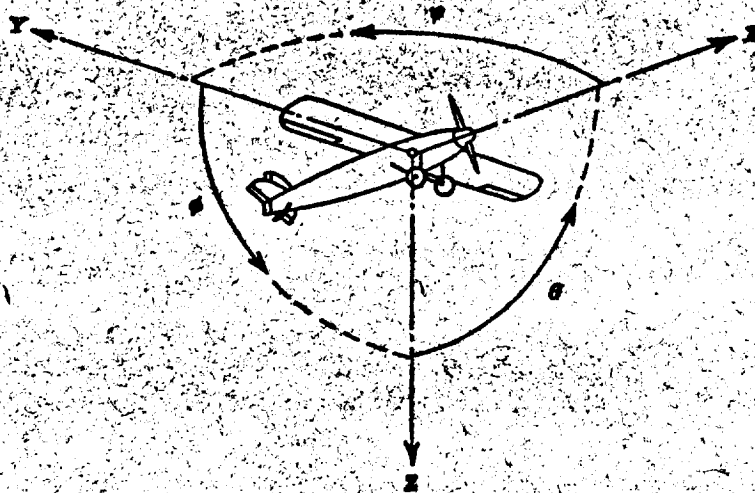
$C_{L_T}$			1.18	1.05	0.92	0.79	2.21	1.96	1.72	1.47	2.59	2.30	2.02	1.73	2.59	2.30	2.02	1.73
Case	W/S	W/hp.	Condition I				Condition II				Condition III				Condition IV			
I	10	8	733	641	646	702	480	420	420	446	447	403	405	432	531	407	394	410
II	10	12	908	889	964	1,106	669	644	665	722	731	690	700	762	713	640	637	672
III	10	16	1,234	1,280	1,427	1,685	1,164	1,086	1,097	1,174	1,197	1,480	1,371	1,463	1,449	1,201	1,111	1,127
IV	20	8	1,331	1,246	1,307	1,472	834	767	796	878	775	734	766	854	888	725	731	792
V	20	12	1,744	1,807	2,047	2,472	1,206	1,202	1,285	1,458	1,400	1,322	1,385	1,601	1,268	1,179	1,205	1,329
VI	20	16	2,533	2,781	3,322	4,374	1,459	1,203	1,258	1,641	1,450	1,450	1,408	1,983	1,481	1,270	1,296	1,393
VII	30	8	2,019	1,967	2,103	2,385	1,251	1,209	1,284	1,445	1,200	1,182	1,265	1,446	1,285	1,134	1,175	1,303
VIII	30	12	2,683	2,879	3,356	4,215	1,812	1,838	2,005	2,341	2,322	2,116	2,239	2,693	1,933	1,802	1,864	2,105

1. 1. 4 Transition assumption not satisfied. Number signifies approximate percentage correction, additive to tabulated run.

TABLE XIV  
COMPUTED GROUNDS RUNS IN FEET

$C_{L_T}$			1.18	1.05	0.92	0.79	2.21	1.96	1.72	1.47	2.59	2.30	2.02	1.73	2.59	2.30	2.02	1.73
Case	W/S	W/hp.	Condition I				Condition II				Condition III				Condition IV			
I	10	8	287	327	382	459	152	174	202	243	136	156	184	224	130	149	173	208
II	10	12	444	511	604	739	235	271	319	392	217	254	305	386	202	233	275	337
III	10	16	635	737	879	1,083	341	399	476	598	331	397	496	690	296	346	415	523
IV	20	8	698	800	939	1,135	369	424	496	601	334	387	458	567	317	364	425	516
V	20	12	1,088	1,267	1,521	1,909	568	663	788	985	525	635	779	1,030	489	570	679	859
VI	20	16	1,577	1,870	2,311	3,062	821	972	1,187	1,557	822	1,009	1,351	2,275	710	843	1,033	1,368
VII	30	8	1,244	1,420	1,655	1,983	677	779	909	1,103	625	728	865	1,079	585	673	787	956
VIII	30	12	1,865	2,192	2,666	3,424	965	1,131	1,359	1,727	922	1,109	1,390	1,901	830	974	1,171	1,491





Positive directions of axes and angles (forces and moments) are shown by arrows

Axis		Force (parallel to axis) symbol	Moment about axis			Angle		Velocities	
Designation	Symbol		Designation	Symbol	Positive direction	Designation	Symbol	Linear (component along axis)	Angular
Longitudinal	X	X	Rolling	L	Y → Z	Roll	$\phi$	u	P
Lateral	Y	Y	Pitching	M	Z → X	Pitch	$\theta$	v	q
Normal	Z	Z	Yawing	N	X → Y	Yaw	$\psi$	w	r

Absolute coefficients of moment

$$C_l = \frac{L}{q b S}$$

(rolling)

$$C_m = \frac{M}{q c S}$$

(pitching)

$$C_n = \frac{N}{q b S}$$

(yawing)

Angle of set of control surface (relative to neutral position),  $\delta$ . (Indicate surface by proper subscript.)

#### 4. PROPELLER SYMBOLS

$D$ , Diameter

$p$ , Geometric pitch

$p/D$ , Pitch ratio

$V_i$ , Inflow velocity

$V_\infty$ , Slipstream velocity

$T$ , Thrust, absolute coefficient  $C_T = \frac{T}{\rho n^3 D^4}$

$Q$ , Torque, absolute coefficient  $C_Q = \frac{Q}{\rho n^3 D^5}$

$P$ , Power, absolute coefficient  $C_P = \frac{P}{\rho n^3 D^5}$

$C_{ps}$ , Speed-power coefficient =  $\sqrt{\frac{\rho V_i^3}{P n^3}}$

$\eta$ , Efficiency

$n$ , Revolutions per second, r.p.s.

$\phi$ , Effective helix angle =  $\tan^{-1} \left( \frac{V}{2\pi r n} \right)$

#### 5. NUMERICAL RELATIONS

1 hp. = 76.04 kg-m/s = 550 ft-lb./sec.

1 metric horsepower = 1.0132 hp.

1 m.p.h. = 0.4470 m.p.s.

1 m.p.s. = 2.2369 m.p.h.

1 lb. = 0.4536 kg.

1 kg = 2.2046 lb.

1 mi. = 1,609.35 m = 5,280 ft.

1 m = 3.2808 ft.

